AIAA JOURNAL
Vol. 30, No. 9, September 1992

Exploratory Study of Wall Pressure Fluctuations in a Mach 5, Sharp Fin-Induced Turbulent Interaction

Berry T. Gibson* and David S. Dolling†
University of Texas at Austin, Austin, Texas 78712

Fluctuating surface pressure measurements have been made near separation in a Mach 5, swept shock/turbulent boundary-layer interaction induced by a sharp fin at angles of attack of 16 and 18 deg. Pressure signals in the initial compression region indicate a "shuddering" compression system, in contrast to a translating separation shock reported in previous studies of sharp fin interactions at Mach 3. The results suggest that the frequency range of the shuddering may scale on the large-eddy frequency of the incoming boundary layer. All of the present results are, within engineering accuracy, consistent with the view that quasiconicity is the salient feature of the interaction footprint. No other topography (e.g., cylindrical) describes the results as well.

Introduction

IT has been known for some time that all shock-wave/turbulent boundary-layer interactions exhibit some degree of unsteadiness. Most of the recent knowledge has come from measurements of fluctuating wall pressures with considerable attention focused on the separation shock-wave motion. A recent review is presented in Ref. 1. In general, the external, inviscid shock wave is stationary. However, in the viscous interaction region within the boundary layer, the bifurcated shock foot may undergo large-scale motion causing intense, intermittent pressure fluctuations on the surface. In interactions induced by compression ramps,[2,3] steps,[4] circular cylinders,[5] and blunt fins[6] it has been shown that the separation shock motion is low frequency (relative to the large eddy frequency U_∞/δ) and broadband (typically 100 Hz–3 kHz). The streamwise extent of the motion L_s is also large. L_s does not appear to scale on δ, but typically spans the region from the upstream influence line to the separation line (as indicated by surface tracer patterns). In the case of compression ramp flows[7] and the axisymmetric analog generated by a cylinder flare,[8] the separated bubble expands and contracts like a balloon, with the instantaneous separation point approximately coincident with the translating separation shock foot.

A recent advance in flowfield visualization has made it possible to obtain video images of fin-generated shock-wave/boundary-layer interactions. By taking advantage of the natural quasiconical symmetry of the interaction, Alvi and Settles[9] were able to capture details of the flow structure using white-light conical shadowgraphy. Pertinent to the present study was their observation of "an inherent 'trembling' unsteadiness of the interaction." However, due to the low framing rate of the video equipment used, this unsteadiness could only be examined qualitatively. In fact, nearly all of the flows in which quantitative data have been obtained are either nominally two-dimensional (i.e., ramps, steps, etc.) or quasi two-dimensional (i.e., on centerline upstream of circular cylinders, blunt fins, etc.). The only exception known to the authors is the work of Tran and his colleagues,[10,11,12] in which fluctuating wall pressure measurements were made along two streamwise rows in a Mach 3 interaction generated by a sharp fin at angle of attack (α = 10, 12, 16, 20 deg). The model configuration, coordinate system, and pertinent features of the interaction footprint are shown in Fig. 1, a and b. Tran[10] concluded that the swept separation shock underwent large-scale motion for angles of attack greater than 12 deg. However, upon close examination of the pressure time histories and probability density distributions reported in Ref. 10, the authors find it difficult to agree with Tran's conclusion. In all interactions characterized by unsteady separation shocks that have been studied thus far, the peak in pressure fluctuation rms has been shown to be a direct result of large-scale, intermittent shock motion, and at the position of the peak rms the probability distribution is bimodal due to the steplike character of the pressure signal. However, in the pressure time histories reported by Tran, the point of maximum rms occurs downstream of any unsteady shock activity and the probability density distribution is almost Gaussian. Although Tran obtained new and interesting results, many fundamental questions could not be answered by his data. Some of these are discussed below.

The present study was intended as a first step in quantifying the unsteadiness of a Mach 5 turbulent interaction generated by a sharp fin at angle of attack. The model arrangement is essentially the same as Tran's but the transducer layout takes advantage of the quasi-conical structure of sharp fin flowfields. The specific questions of interest included:

1) Is intermittent separation a feature of nominally two-dimensional flows only, or is it also a feature of highly swept, separated flowfields? If intermittent separation does occur, does it remain intermittent at all radial stations, or far from the fin leading edge, where the flowfield length scales are very large, is the nominally steady model of separation with a distributed compression fan essentially correct?

2) How do the separation shock dynamics vary radially? In two-dimensional flows the upstream influence and separation lines which are the boundaries of the shock motion are parallel, whereas in quasiconical flows they lie along rays and therefore diverge radially (Fig. 1). If the same physical model holds as in two-dimensional flows, and the shock does translate between β_{ui} and β_{S_1} then the length scale of the shock motion would increase linearly radially. This raises the intriguing questions of how the shock frequencies and speeds would vary as the shock length scale increases.

However, due to the unanticipated findings of this study, these original questions had to be modified as explained in the discussion of the results.

Received Aug. 31, 1990; presented as Paper 91-0646 at the AIAA 29th Aerospace Sciences Meeting, Reno, Nevada, January 7–10, 1991; revision received Aug. 12, 1991; accepted for publication Aug. 19, 1991.

*Graduate Research Assistant, Department of Aerospace Engineering and Engineering Mechanics; currently with the Advanced Technology and Design Center of the Northrop Corporation, Pico Rivera, CA. Member AIAA.

†Associate Professor, Department of Aerospace Engineering and Engineering Mechanics. Associate Fellow AIAA.

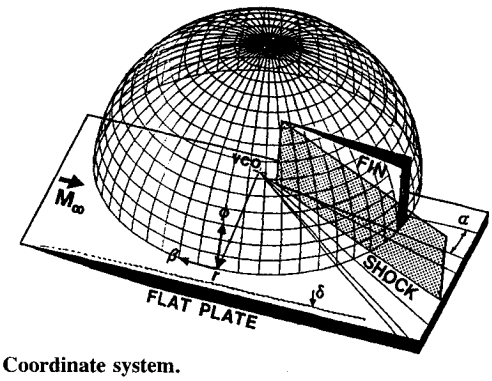

Fig. 1a Coordinate system.

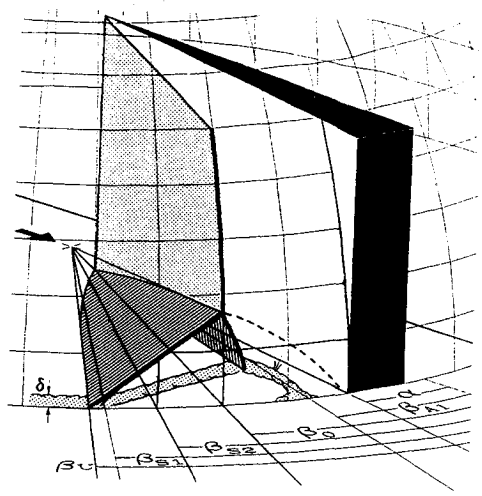

Fig. 1b Projection of quasiconical interaction onto spherical coordinate surface.

Experimental Program

The following is only a brief overview of the experimental program. For more details, the reader is referred to Ref. 13.

Flow Conditions and Model Description

All experiments were conducted in the Mach 5 blowdown tunnel of the University of Texas at Austin with nominal freestream properties as given in Table 1.

As shown in Fig. 2, a 30-in.-long (76.2 cm), full-span flat plate was mounted horizontally 3 in. (7.6 cm) above the tunnel floor. A 5.25-in.-diam (13.3 cm) hole, centered 22.1 in. (56.1 cm) from the leading edge, accommodated a rotatable, brass instrumentation plug which was machined flush with the surface of the flat plate. A vacuum seal was maintained between the upper surface of the plug/flat plate and the lower surface of the coverplate/flat plate junctions. The shock waves were generated by an unswept, sharp leading edged, stainless steel fin installed normal to the test surface. The fin dimensions were such that a dimensionless, semi-infinite, swept interaction was produced over the span of the test section. Because of tunnel starting problems at high angles of attack, a mechanism was designed that would allow the fin angle to be varied from a low value, for tunnel startup, to the desired test angle after supersonic flow had been established. The fin's angle was controlled by a translating arm pinned to the fin's leeward side. Due to a slight hysteresis effect in the threads, the accuracy of the angle of attack is estimated to be within ± 0.2 deg.

All fluctuating surface pressure measurements were made using transducers mounted flush with the surface of the instrumentation plug. The arrangement of the transducer ports, shown in Fig. 3, was based on the empirical correlation for upstream influence angle developed by Lu et al.[14] and the virtual conical origin (VCO) data of Lu and Settles.[15] The instrumentation plug used throughout the experiments was optimized for $\alpha = 18$ deg. The methodology for selecting transducer port locations was as follows.

The virtual origin position was located 0.50 in. (1.3 cm) from the fin apex along the trace of the inviscid shock wave.

Table 1 Incoming flow conditions

M_∞	4.95	4.95
U_∞	790 m/s	2600 ft/s
P_0	2.17 MPa	315 psia
T_0	374 K	673°R
Re_∞	44.6×10^6/m	13.6×10^6/ft

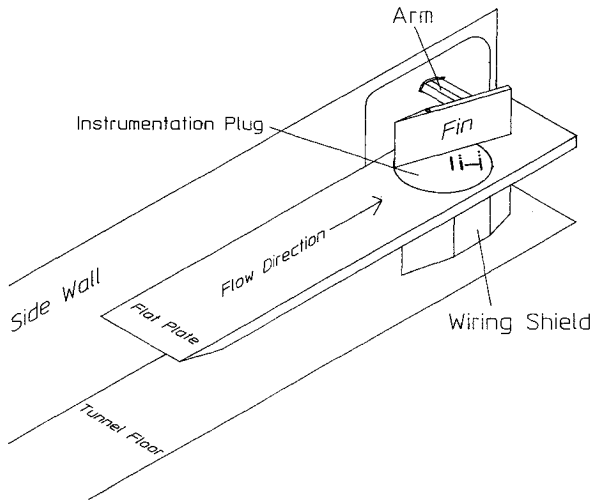

Fig. 2 Model configuration.

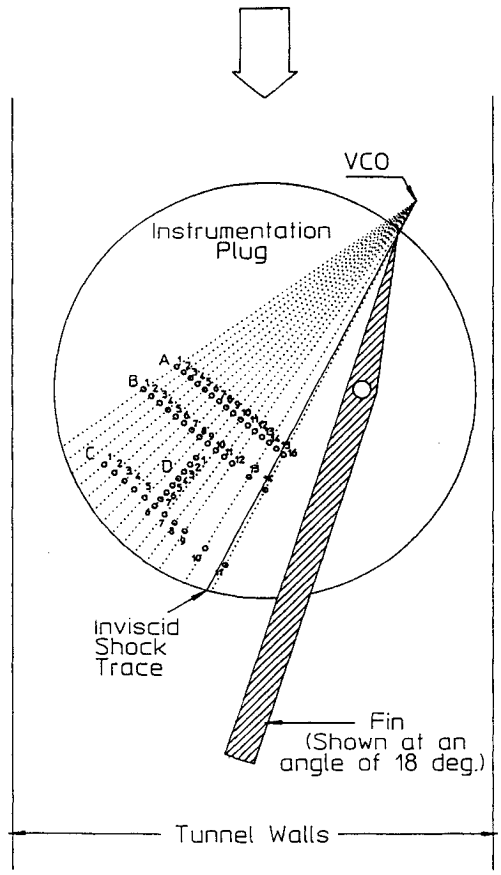

Fig. 3 Transducer arrangement.

Lu et al.[14] showed that a reduced upstream influence angle, $\Delta\beta_{ui} = (\beta_{ui} - \mu_\infty)$, scales with a reduced shock angle, $\Delta\beta_0 = (\beta_0 - \mu_\infty)$, for $M_\infty = 2.5$–4 and $\Delta\beta = 0$–20 deg. An empirical fit of the data took the form

$$\Delta\beta_{ui} = 2.2\Delta\beta_0 - 0.027\Delta\beta_0^2 \quad (1)$$

Thus, from Eq. (1) the upstream influence line was predicted to lie at 40 deg to the freestream. Transducer ports were positioned along straight lines denoted by A, B, C, and D in Fig. 3. Lines A, B, and C are perpendicular to the predicted upstream influence line and survey line D lies along the predicted upstream influence line. To take advantage of the quasiconical nature of the interaction, corresponding transducer locations on A, B, and C lie along conical rays passing through the virtual origin. In a purely conical reference frame, the survey lines should be along circular arcs centered at the VCO, but since the majority of data was taken in a small region bounded approximately by β_u and β_0, the "error" incurred by using straight lines is not significant.

Instrumentation

Surface pressure fluctuations were measured with up to eight absolute pressure transducers (model XCQ-062-50A) made by Kulite Semiconductor Products, Inc. Each transducer has a 0.028-in.-diam (0.071 cm) sensing diaphragm that is protected by an outer screen having a nominal outer diameter of 0.064 in. (0.16 cm). The pressure range is 0–50 psia (0–0.345 MPa) and the effective frequency response is about 50 kHz. The Kulite company claims a thermal zero shift of 2% full scale/100°F (1 psi/100°F). Consequently, due to the increasing temperature of the transducers during a run (about 20 s expired between tunnel startup and data acquisition), the mean values were not reliable. The transducer sensitivity, however, was not affected; thus, pressure fluctuations could be measured accurately. The short duration of the data acquisition, typically of order 1 s, resulted in a reasonably constant, albeit inaccurate, mean for the data set.

The transducer signals were amplified and then low-passed filtered, at the lower of 50 kHz or half the sampling rate, by Ithaco model 4113 or model 4213 analog filters. An A/D converter with sample-and-hold digitized the filtered signals at rates up to 500 kHz, depending on the number of simultaneously sampled transducers and time resolution required. The maximum amount of data possible was obtained, and was equal to (800 records)/(no. of channels sampled). A record comprised 1024 data points.

Test Procedure

The test program comprised four phases. In phase 1 Pitot profiles of the boundary layer were obtained at 18.9 in. (48.0 cm) from the flat-plate leading edge: on centerline ($z = 0$) and 1.5 in. (3.8 cm) to each side of centerline. The survey line was about 1.2 in. (3.0 cm) upstream of the leading edge of the fin. The experimental data were fitted by the method of least squares to the wall-wake velocity profile developed by Sun and Childs.[16] The results are provided in Table 2.

Table 2 Undisturbed boundary-layer parameters

Parameter	$z = -1.5$ in. (−3.81 cm)	$z = 0$ in. (0 cm)	$z = +1.5$ in. (+3.81 cm)
δ_0	0.24 in. (6.1 mm)	0.20 in. (5.08 mm)	0.24 in. (6.1 mm)
δ^*	0.12 in. (3.05 mm)	0.099 in. (2.51 mm)	0.12 in. (3.05 mm)
θ	0.0098 in. (0.25 mm)	0.0083 in. (0.21 mm)	0.0098 in. (0.25 mm)
Re_θ ($\times 10^{-3}$)	11.5	9.08	11.0
C_f ($\times 10^4$)	9.52	10.3	9.60
Π	0.452	0.409	0.483

The results indicate a fully turbulent, zero pressure gradient boundary layer. However, the boundary layer cannot be characterized as truly two-dimensional. It is known that two-dimensional nozzles tend to induce an adverse pressure gradient across the sidewalls of the divergent section, thus causing the sidewall boundary layer to thicken in the middle. The interaction of this bulge in the sidewall boundary layer with the boundary layer on the flat plate is a probable cause for the increase in δ_0 off centerline. The "straightness" of the separation line from flow visualization tests would seem to indicate that radial variations in boundary-layer thickness of this magnitude have little effect on the interaction.

In phase 2 of the experiment, fluctuating pressure measurements were made to obtain the rms, power spectral density, coherence function, convection velocity, and so on, of the undisturbed, incoming boundary layer. The data were obtained along streamwise and transverse survey lines using two or three simultaneously sampled transducers with spacings ranging from 0.57 δ_0 to 4.6 δ_0. From an average of 20 transducer samplings over nine tests, the rms of the pressure fluctuations in the undisturbed, incoming boundary layer was determined to be $\sigma_{p0} = 0.010$ psia. The standard deviation of the set of 20 rms calculations was 0.001 psi. Normalized by freestream dynamic pressure and wall shear stress, the values of σ_p/q_w and σ_p/τ_w are 9.25×10^{-4} and 0.893, respectively. These values are somewhat low compared with the results of other investigators.[1] This can be attributed to spatial integration, due to the physical size of the transducer relative to the thin boundary layer, which acts as a low-pass filter, thus eliminating the contributions from high frequencies. Since the focus of this study is on the higher amplitude, lower frequency fluctuations in the interaction, this limitation is not a serious constraint.

In phase 3, surface flow visualization tests were conducted to identify interaction surface features and to evaluate the empirical upstream influence correlation of Lu et al.[14] A permanent record of the surface flow features was obtained by employing a variation of the kerosene-lampblack method. Diesel fuel was added to the slurry to lower its volatility. Surface patterns were obtained for fin angles of attack of 10.5 and 15 deg, but the image quality was poor and accurate angular measurements were not possible. Results for higher angles were precluded by the premature drying of the slurry before the test angle had been reached.

In phase 4, fluctuating surface pressure measurements were made within the interaction at 16 deg $\leq \alpha \leq$ 21 deg. Up to eight transducers along survey lines A, B, and C (Fig. 3) were simultaneously sampled at 110–160 kHz for $\alpha = 16$ and 18 deg. The objective of these runs was to identify the boundary between undisturbed boundary-layer flow and the initial compression. Once this boundary was determined, transducers along the survey lines were simultaneously sampled, two at a time, at 500 kHz. In addition, seven transducers along the approximate conical ray D were simultaneously sampled at 120 kHz for $\alpha = 16$ and 18 deg.

Discussion of Results

Characteristics of Wall Pressure Signals

Sample pressure signals in the undisturbed boundary layer and in the region of the initial compression are shown in Fig. 4, a and b, for $\alpha = 18$ deg. Corresponding plots of the probability density distributions (PDDs) are shown beneath in Fig. 4, c and d. Even though the rms of the signal in Fig. 4b has not yet risen significantly above that of the undisturbed boundary layer, the probability density distribution in Fig. 4d is slightly skewed compared to the Gaussian distribution of Fig. 4c. This is due to weak compressions superimposed on the undisturbed boundary-layer signal. However, it is obvious that the pressure signal is not intermittent, and the skewness

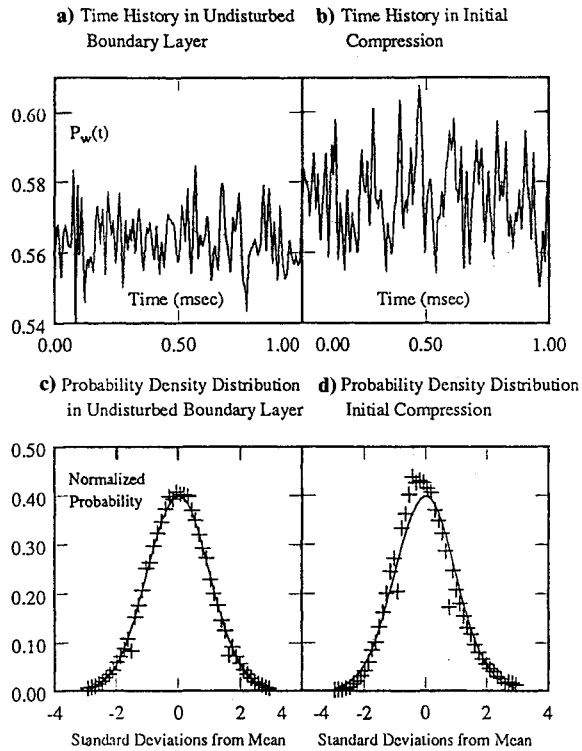

Fig. 4 Pressure signals and corresponding probability density distributions.

is small compared to the results of Tran and those from two-dimensional and quasi-two-dimensional interactions.

The two specific questions raised in the Introduction arose from the work of Tran, who claimed that the wall pressure signals near separation were intermittent and indicative of an unsteady separation shock foot. However, the wall pressure fluctuations measured in the current study have revealed a different flow structure than was anticipated from Tran's work. At all angles of attack studied, which included those generating extensive separated flow (as indicated by surface flow visualization), the wall pressure signals near separation showed *no evidence of intermittency* (i.e., *no evidence of a translating separation shock*). In fact, the results of the present study led the authors to re-evaluate the conclusions drawn by Tran (as mentioned in the Introduction). Thus, the data answer the first part of question 1 in the Introduction and render question 2 (concerning the shock dynamics) inappropriate. However, they raise new and important questions about the apparent "universal nature" of the unsteadiness of shock-induced turbulent separation and how it is affected by sweepback. The revisions to those questions posed in the Introduction include:

1) If the separation shock in a Mach 3 fin interaction undergoes large-scale, low-frequency motion, why is there a comparatively steady compression system in a considerably stronger Mach 5 interaction at similar angles of attack? Is shock strength an important factor in determining the degree of unsteadiness? Does the large-eddy frequency U_∞/δ of the incoming boundary layer affect the unsteadiness? In swept interactions is the degree of sweep important?

2) How do the flowfield dynamics vary radially? Do rms distributions and power spectral densities develop quasiconically in the same way as the mean wall pressure, or are there changes in the dynamics that are not reflected in the mean values?

The answers to some of these questions are presented in this paper, but further studies are required over a wider range of parameters, including M, α, and δ_0, to answer them all satisfactorily.

Rms Distributions

Figure 5 shows the distribution of the rms σ_p of the wall pressure fluctuations along the three survey lines oriented approximately normal to the upstream influence line β_{ui} for α = 18 deg. The open symbols represent data obtained with sampling rates < 140 kHz, and the shaded symbols denote 500-kHz data. The solid lines were hand-drawn to clearly show the trends. The data are shown in absolute units because neither the local mean value nor the undisturbed boundary-layer rms level could be measured accurately as explained earlier. The scatter in the rms at particular locations is typical when such low-amplitude pressure fluctuations are measured by 0–50-psia transducers. The abscissa is the distance from the point of intersection of the survey line with the inviscid shock trace to the sampling position nondimensionalized by the boundary-layer thickness. Note the rapid rise in rms marking the initial compression and the absence of a well-defined rms peak (whose presence usually indicates an unsteady shock foot). If the flowfield were cylindrically symmetric, the distributions would collapse in this coordinate system. However, since this is not the case, they were replotted in an angular coordinate system (centered at the VCO as in Fig. 1). As shown in Fig. 6, the rms distribution at different radial distance collapse reasonably well. Thus, the rms distributions *appear* to exhibit quasiconical symmetry. However, to qualify

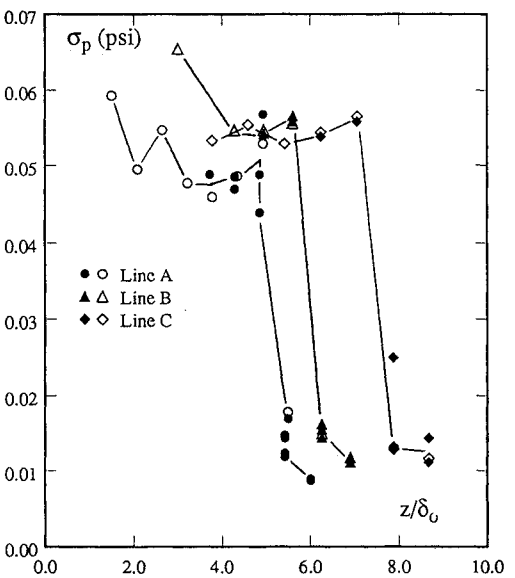

Fig. 5 Rms pressure distributions, α = 18 deg.

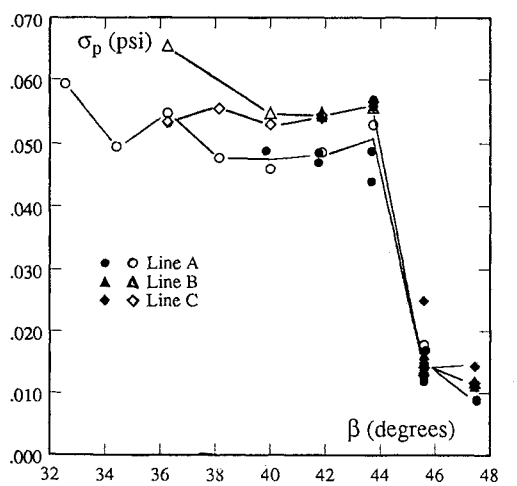

Fig. 6 Rms pressure distributions in conical coordinates, α = 18 deg.

this statement, it should be noted that, given the low levels of pressure fluctuations through the present interactions, the resulting scatter in the rms at particular locations precludes a categorical conclusion of quasiconical symmetry.

Upstream Influence Angle Correlation

Upstream influence is usually defined as the point at which the mean wall pressure first rises above the undisturbed boundary-layer level. A corollary to this definition, using the location of initial rms rise, typically places it only slightly further upstream. Table 3 shows upstream influence angle β_{ui} for α = 16–20 deg determined from plots of σ_p vs β. As expected, β_{ui} increases with α. However, comparisons made with the results from the β_{ui} correlation given by Eq. (1) and presented in Table 3 provide some interesting observations. Upstream influence angles determined from the initial rms rise are 5–8 deg larger than those from the correlation based on surface tracer patterns.

In the absence of surface flow visualization results, the upstream influence location can also be determined from a plot of the mean wall pressure by constructing a tangent to the maximum gradient of the initial pressure rise and noting the intersection with the undisturbed boundary-layer level. From Rodi's[17] mean wall pressure distribution shown in Fig. 7, β_{ui} was determined to be 42 deg for a 16-deg interaction under virtually the same conditions as studied in the present investigation. This agrees well with the value for β_{ui} found from the initial rms rise. Thus, the correlation developed by Lu et al.[14] from data taken in the Pennsylvania State University Supersonic Wind Tunnel for Mach numbers up to 4 cannot be extrapolated to predict the results in the present facility at Mach 5. The experiments in the Penn State tunnel were performed with similar boundary-layer thicknesses, but at higher Reynolds numbers; however, Reynolds number effects on β_{ui} are small. More tests under a wider range of conditions are needed to develop a more universal correlation (if one exists). Thus, if using empirical correlations when flow visualization is not available, future investigators should make appropriate provisions in their transducer layout.

Table 3 Upstream influence angles vs angle of attack

α, deg	(β_{ui}) from rms rise, deg.	(β_{ui}) from correlation, deg
16	43–44	37
18	45–46	40
19	47.5–48.5	41.5
20	50–51	43

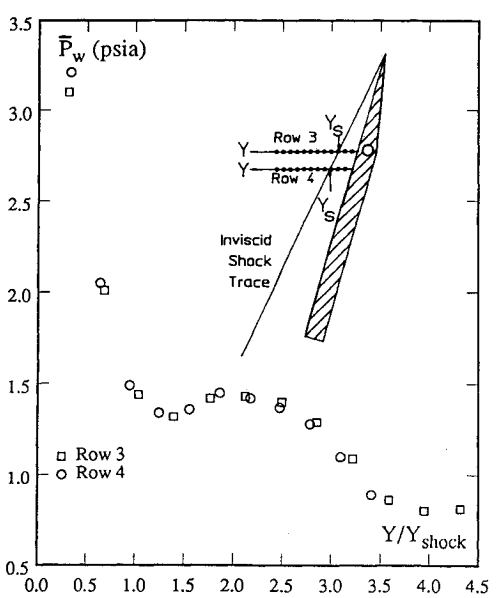

Fig. 7 Mean surface pressure distribution measured by Rodi;[17] M_∞ = 5, α = 16 deg.

Power Spectral Densities

Normalized power spectra at four different positions along the middle survey line from the 18-deg interaction are shown in Fig. 8. The frequency content of the incoming boundary layer, curve 1, is broadband, with most of the energy above 15 kHz. The transducer generating curve 2 is just within the initial compression, and in addition to a boundary-layer-type signature, there is now significant contribution from lower frequencies in the range of 4–12 kHz. Curve 3, completely within the compression region, shows that the signal is now dominated by the lower frequency fluctuations induced by the "shuddering" of the compression system. The compression system appears to be relatively disperse, extending over two transducer stations. In addition to the lower frequency content of the spectra, these two stations were distinguished by slightly skewed PDDs. In the "plateau" region of the rms distribution (curve 4), the energy content shifts toward the high-frequency range again (4–40 kHz), but note that the lower frequencies still persist. Similar behavior is observed under the separated shear layer in two-dimensional interactions.[1] At stations even further down the survey line (not shown), the lower frequency content tends to diminish and the PDDs are again Gaussian.

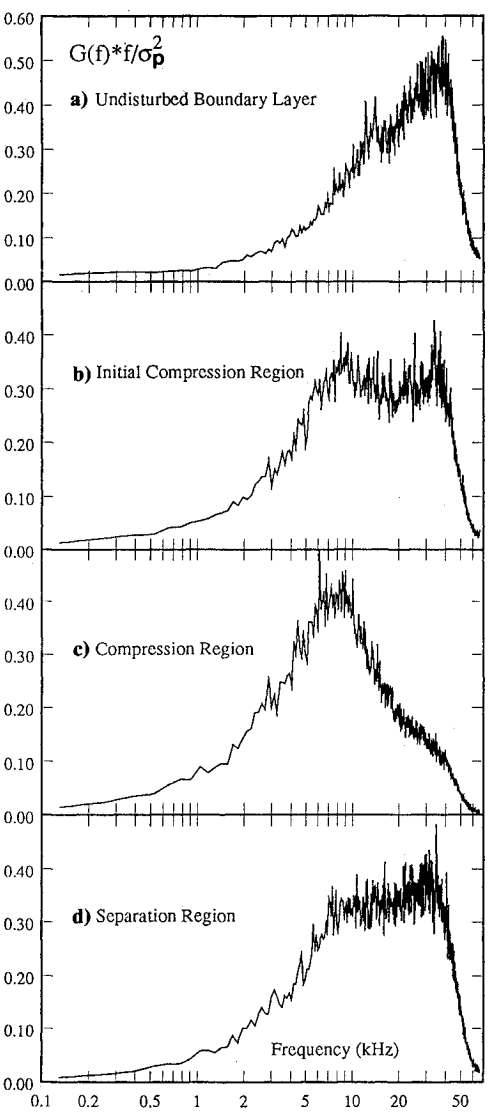

Fig. 8 Evolution of power spectra along row B, α = 18 deg.

For all angles of attack tested, the characteristic frequencies at corresponding interaction locations (initial rms rise, maximum rms, plateau rms, etc.) were virtually identical.

Figure 9 shows the contribution of four frequency ranges to the signal variance along the middle survey line in the 18-deg interaction. The abscissa is the conical angle β such that the farthest position to the right is in the undisturbed boundary layer, the next is at the initial compression, and so forth. The first four positions (from right to left) correspond to the four power spectra of Fig. 8. The fraction of the variance in each frequency band sums to unity since

$$\sigma^2_{f1f2} = \int_{f1}^{f2} G(f)\, df$$

and therefore

$$\int_{f1}^{f2} \frac{G(f) * f}{\sigma^2_{f1f2}}\, d(\ell n f) = 1$$

It is evident that the major contribution in the undisturbed boundary layer is from frequencies in the 15–50-kHz range, as expected. In the initial compression the contribution from the high-frequency range decreases to about the same level as that from the compression system "shuddering," in the 5–15-kHz range. In addition, the contributions from the two low-frequency bands begin to increase. At the third position, completely within the compression, the fraction in the 15–50-kHz range has dropped sharply, while the 5–15-kHz band peaks to become the major contributor to the signal variance. The two low-frequency bands peak also. In the separated flow the high-frequency band (15–50 kHz) contribution increases sharply to the undisturbed boundary-layer level. The contributions from the other three bands decrease. The most noteworthy observation here is that the contributions from all four frequency bands approach about the same proportions they had in the undisturbed boundary layer. Thus, it appears that the incoming turbulence passes through the compression system with virtually no net change in the frequency content.

The power spectra in the compression region are different from those found by Tran[10] at Mach 3 and markedly different from those found in the intermittent region of two-dimensional interactions. In the present experiment, characteristic frequencies of the compression system unsteadiness were centered around 8 kHz and were relatively broadband. Tran observed a relatively broadband of frequencies, but centered around 2 kHz. In two-dimensional interactions a fairly narrow band of frequencies has been observed in the intermittent region with center frequencies of 1 kHz or less.

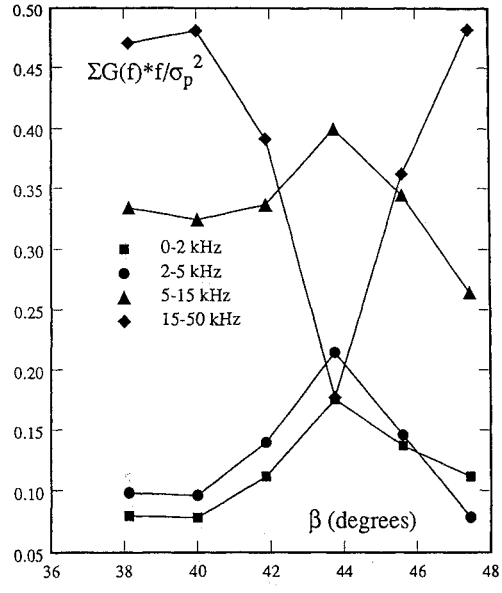

Fig. 9 Fraction of variance in four frequency bands along row B, α = 18 deg.

In Tran's experiment, the ratio U_∞/δ_0, which is a representative frequency of the large-scale eddies, was about 33 kHz. For the Mach 5, flat-plate boundary layer, $U_\infty/\delta_0 \approx 150$ kHz. If the unsteadiness of the compression system shock is induced or influenced by turbulent structures in the incoming boundary layer, one might expect the frequency of this unsteadiness to correlate with the frequency of the structures. To explore this point further, consider that the ratio of U_∞/δ_0 for the two cases is about 4.5:1 and that the ratio of the compression system shock center frequencies is about 4:1. The similarity of these ratios suggests that there may be some correlation. From fluctuating pressure measurements in the intermittent region of an unswept compression ramp interaction, Erengil and Dolling[18] observed that the separation shock undergoes a large-scale, low-frequency motion with a superposed high-frequency "jitter." While the mechanism driving the low-frequency motion was not identified, it was concluded that the high-frequency "jitter" correlated with the passage of specific large-scale structures in the incoming flow. In the same compression ramp interaction, it was also found that the large-amplitude, low-frequency component of the pressure signals under the separated shear layer were correlated with the low-frequency, large-scale motion of the shock.[3] However, it could not be determined which was the cause and which was the effect. In light of the recent observations by Erengil and Dolling, the tentative results of the present study may offer some insight into the mechanism(s) driving the unsteadiness in turbulent interactions. Although a direct connection has not yet been established, it is possible that the two different types of simultaneous shock motion (low-frequency, large-scale and high-frequency "jitter") are related to two separate phenomena (separation-induced pressure fluctuations operating through a feedback mechanism and incoming turbulent fluctuations, respectively).

By virtue of the "sweep" of fin-induced interactions, the separated flow is incapable of significantly affecting the separation shock or compression system on a global scale. On the other hand, the strong, subsonic flow reversal in two-dimensional interactions provides an effective mechanism for feedback of separation-induced pressure fluctuations to the separation shock. Therefore, *if* large-scale, low-frequency shock motion is the result of separation-induced pressure fluctuations, it is possible that swept, and particularly highly swept, interactions may exhibit unsteadiness controlled primarily by incoming, turbulent fluctuations. This would explain the existence of a compression system which "jitters" or "shudders" at high frequencies in a Mach 5 fin interaction. For similar angles of attack and thus less "sweep," it would also account for the lower, but still relatively high, frequencies in a Mach 3 interaction.

One of the objectives was to determine how the dynamics of the compression system varied radially. Figure 10 shows power spectra for the 16-deg interaction at three radial stations which lie along a conical ray from the VCO. All stations are in the region of rapid rms rise. Note that the spectra are virtually identical. In fact, this result was confirmed for *any three radial stations positioned along a conical ray in the entire interaction region and for all shock strengths tested.* Visually, the spectra along conical rays appear invariant. Close examination reveals small changes in the contributions from particular frequency ranges as seen in Fig. 11. The figure shows the contribution of four frequency bands to the variance of the signals whose spectra are shown in Fig. 10. The abscissa is the radial distance from the VCO to the measuring station nondimensionalized for convenience by the boundary-layer thickness. At each position the primary contribution to the variance is from the compression system "shuddering," in the

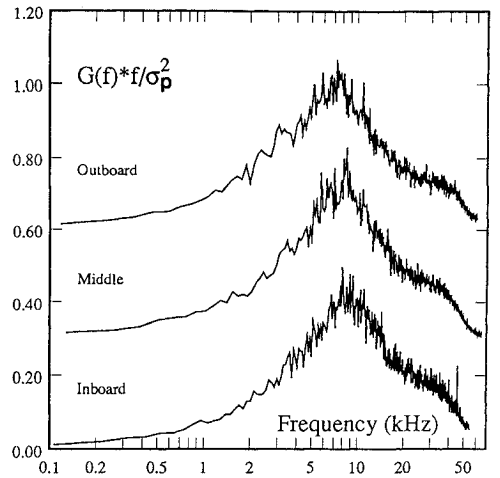

Fig. 10 Radial variation of power spectra in compression region of 16-deg interaction (middle and outboard curves are each shifted 0.3 unit of $G(f) \cdot f/\sigma_p^2$ upwards).

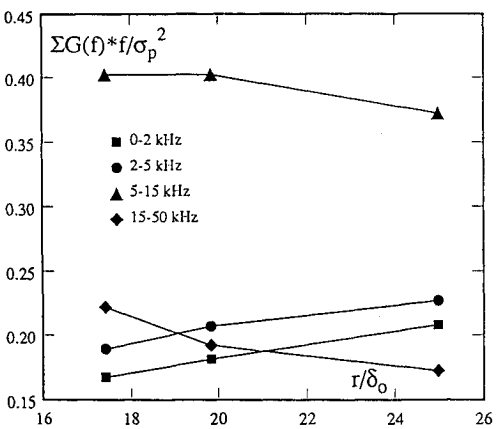

Fig. 11 Fraction of variance in four frequency bands along a conical ray in compression region, α = 16 deg.

5–15-kHz range. The results show a gradual increase of the contributions from the two low-frequency bands with radial distance from the fin, suggesting a subtle evolution of the energy content in given frequency ranges of the compression system unsteadiness with increasing radial distance. Since the undisturbed boundary layer thickens radially (due to the non-two-dimensionality discussed previously, in addition to regular streamwise growth), the large-eddy frequency would decrease. Consequently, if the compression system unsteadiness is related to the incoming large-eddy frequency, it is consistent that the "shuddering" becomes lower in frequency. On the other hand, it is quite possible that any misalignment between row D and a true ray could generate this result and thus the physical interpretation above must be treated with caution. Additional experiments are needed to clarify the issue.

Summary

Fluctuating wall pressures have been measured near separation in a Mach 5, sharp fin-induced turbulent interaction. The majority of data was obtained with fin angles of attack of 16 and 18 deg. High-frequency response pressure transducers were positioned to take advantage of the quasiconical symmetry of the flowfield. The original objective was to study the radial evolution of the swept separation shock dynamics. However, the fluctuating pressure signals in the initial compression region indicate the presence of a disperse compression wave "shuddering" above, in contrast to a translating separation shock purported by earlier researchers in the same type of interaction at Mach 3. Nevertheless, several features of this Mach 5 interaction are in qualitative agreement with those found at Mach 3. Furthermore, the present study has extended earlier work to include variations with radial distance. However, the most salient feature of this interaction is its *degree of steadiness*. The following conclusions support this claim and summarize the results presented in this paper:

1) Wall pressure signals near separation showed no evidence of intermittency. Visual inspections of the raw data and slight skewness in the probability density distributions upstream of separation indicates the presence of weak compressions superimposed on the undisturbed boundary-layer signal.

2) All rms distributions exhibit a rapid rise marking the initial compression upstream of separation. However, unlike a distribution resulting from an unsteady separation shock foot, there is no well-defined rms peak. Within engineering accuracy, the rms distributions appear to collapse in a conical reference frame.

3) There is a difference of 5–8 deg between the upstream influence angles (β_{ui}) determined from the initial rms rise and the upstream influence angles predicted from the correlation developed in earlier studies. Since β_{ui} from the initial rms rise is in agreement with β_{ui} determined from mean pressure distributions in the same flowfield, confidence can be placed in the measurements. Thus it appears that the earlier correlation, based on data in the Mach number range of 2.5–4.0 may not be viable at higher Mach numbers.

4) Power spectral densities show an evolution from the incoming boundary-layer signature to one dominated by lower frequencies in the range of 4–12 kHz in the compression region. Even though the rms increases with angle of attack, the characteristic frequencies at corresponding interaction locations were virtually identical for all angles of attack tested. Separating the contributions to the variance into four frequency ranges showed virtually no net change in frequency content through the compression system.

5) An argument was developed that might shed light on the mechanisms driving interaction unsteadiness. Due to the sweep of fin-induced interactions, separation-induced disturbances are less likely to affect global shock unsteadiness. Thus, with the primary disturbances coming from the incoming boundary layer, highly swept interactions may be characterized by high-frequency unsteadiness which correlates with the incoming turbulent structure frequency.

6) Visual inspection of power spectral densities shows that they are invariant along conical rays, thus suggesting conical symmetry. In fact, within engineering accuracy, all of the results are consistent with the view that quasiconicity is the salient feature of the interaction footprint. No other topography (e.g., cylindrical) can be found which describes the results as well.

Acknowledgments

This work was funded largely by NASA Langley Grant NAG-1-1005 monitored by William Zorumski. Additional support was provided by The Center for Hypersonics Training and Research at The University of Texas at Austin (Grant NAGW 964, funded by NASA, AFOSR, and ONR). These sources of support are gratefully acknowledged. The suggestions of Gary S. Settles are also gratefully acknowledged.

References

[1]Dolling, D. S., and Dussauge, J. P., "Wall Pressure Fluctuations in Turbulent Flow," *A Survey of Measurements and Measuring Techniques in Rapidly Distorted Compressible Turbulent Boundary Layers*, May 1989, Chap. 8, NATO Agardograph 315.

[2]Dolling, D. S., and Murphy, M. T., "Unsteadiness of the Separation Shock Wave Structure in a Supersonic Compression Ramp Flowfield," *AIAA Journal*, Vol. 21, No. 12, 1983, pp. 1628–1634.

[3]Erengil, M. E., and Dolling, D. S., "Separation Shock Motion and Ensemble-Averaged Wall Pressures in a Mach 5 Compression

Ramp Interaction," AIAA 20th Fluid Dynamics, Plasma Dynamics and Lasers Conf., AIAA Paper 89-1853, Buffalo, NY, June 1989.

[4]Kistler, A. L., "Fluctuating Wall Pressure Under Separated Supersonic Flow," *Journal of Acoustical Society of America*, Vol. 36, March 1964, pp. 543–550.

[5]Dolling, D. S., and Smith, D. R., "Separation Shock Dynamics in Mach 5 Turbulent Interactions Induced by Cylinders," *AIAA Journal*, Vol. 27, No. 12, 1989, pp. 1698–1706.

[6]Dolling, D. S., and Bogdonoff, S. M., "An Experimental Investigation of the Unsteady Behavior of Blunt Fin-Induced Shock Wave Turbulent Boundary Layer Interactions," AIAA Paper 81-1287, June 1981.

[7]Gramann, R. A., and Dolling, D. S., "Dynamics of Separation and Reattachment in a Mach 5 Unswept Compression Ramp Flow," AIAA 28th Aerospace Sciences Meeting, AIAA Paper 90-0380, Reno, NV, Jan. 1990.

[8]Kussoy, M. I., Brown, J.D., Brown, J. L., Lockman, W. K., and Horstman, C. C., "Fluctuations and Massive Separation in Three-Dimensional Shock Wave/Boundary-Layer Interactions," Second International Symposium on Transport Phenomena in Turbulent Flows, Tokyo, Japan, Oct. 25–29, 1987.

[9]Alvi, F. S., and Settles, G. S., "Structure of Swept Shock Wave/Boundary-Layer Interactions Using Conical Shadowgraphy," AIAA 21st Fluid and Plasma Dynamics Conf., AIAA Paper 90-1644, Seattle, June 1990.

[10]Tran, T. T., "An Experimental Investigation of Unsteadiness in Swept Shock Wave/Turbulent Boundary Layer Interactions," Ph.D. Thesis, Mechanical and Aerospace Engineering Dept., Princeton Univ., March 1987.

[11]Tran, T. T., Tan, D. K. M., and Bogdonoff, S. M., "Surface Pressure Fluctuations in a Three-Dimensional Shock Wave/Turbulent Boundary Layer Interaction at Various Shock Strengths," AIAA 18th Fluid Dynamics and Plasmadynamics and Lasers Conf., AIAA Paper 85-1562, Cincinatti, OH, July 1985.

[12]Tan, D. K. M., Tran, T. T., and Bogdonoff, S. M., "Wall Pressure Fluctuations in a Three-Dimensional Shock-Wave/Turbulent Boundary Interaction," *AIAA Journal*, Vol. 25, No. 1, 1987, pp. 14–21.

[13]Gibson, B. T., "An Experimental Study of Wall Pressure Fluctuations Near Separation in a Mach 5, Sharp Fin-Induced Turbulent Interaction," M.S. Thesis, Dept. of Aerospace Engineering and Engineering Mechanics, Univ. of Texas at Austin, Aug. 1990.

[14]Lu, F. S., Settles, G. S., and Horstman, C. C., "Mach Number Effects on Conical Surface Features of Swept Shock Boundary-Layer Interactions," AIAA 19th Fluid Dynamics, Plasma Dynamics and Lasers Conf., AIAA Paper 87-1365, Honolulu, HI, June 1987.

[15]Lu, F. K., and Settles, G. S., "Inception Length to a Fully-Developed Fin-Generated Shock Wave Boundary-Layer Interaction," AIAA Paper 89-1850, June 1989.

[16]Sun, C, and Childs, M. E., "A Modified Wall-Wake Velocity Profile for Turbulent Compressible Boundary Layers," *AIAA Journal*, Vol. 10, No. 6, 1973, pp. 381–383.

[17]Rodi, P. E., private communication, June 1990.

[18]Erengil, M. E., and Dolling, D. S., "Correlation of Separation Shock Motion in a Compression Ramp Interaction with Pressure Fluctuations in the Incoming BoundaryLayer," AIAA 21st Fluid Dynamics, Plasma Dynamics and Lasers Conf., AIAA Paper 90-1646, Seattle, June 1990.